



Preparation of Zn-modified nano-ZSM-5 zeolite and its catalytic performance in aromatization of 1-hexene

Gao-liang WANG¹, Wei WU¹, Wang ZAN¹, Xue-feng BAI¹, Wen-jing WANG¹, Xin QI¹, O.V. KIKHTYANIN²

1. Key Laboratory of Chemical Engineering Process & Technology for High-Efficiency Conversion, School of Chemistry and Materials Sciences, Heilongjiang University, Harbin 150080, China;

2. Borskov Institute of Catalysis, Siberian Branch of the Russian Academy of Sciences, Novosibirsk 630090, Russia

Received 8 January 2014; accepted 5 March 2014

Abstract: The promoting effect of introducing Zn into nano-ZSM-5 zeolites by conventional impregnation method and isomorphous substitution on the performance of 1-hexene aromatization was investigated. The nano-ZSM-5 zeolite was synthesized by a seed-induced method without organic templates. The Zn-modified nano-ZSM-5 zeolite catalysts, $x\text{Zn}/\text{HNZ5}$ and $y\text{Zn}/\text{Al-HNZ5}$, were prepared by the conventional impregnation method and isomorphous substitution, respectively. The structure, chemical composition and acidity of the catalysts were characterized by XRD, XRF, N_2 adsorption, SEM, NH_3 -TPD and Py-IR, while the catalytic properties were evaluated at 480 °C and a weight hourly space velocity (WHSV) of 2.0 h^{-1} in the aromatization procedure of 1-hexene. Compared with $x\text{Zn}/\text{HNZ5}$, $y\text{Zn}/\text{Al-HNZ5}$ exhibited smaller particles and higher dispersion of Zn species, which led to greater intergranular mesopore and homogeneous acidity distribution. Experimental results indicated that the synergy effect between the Brønsted and Lewis acid sites of the isomorphously substituted nano-ZSM-5 zeolites could significantly increase aromatics yield and improve catalytic stability in the 1-hexene aromatization.

Key words: nano-ZSM-5 zeolite; Zn-modification; catalytic performance; isomorphous substitution; aromatization

1 Introduction

ZSM-5 zeolite is a microporous aluminosilicate material with well-defined pore structures and compositions, which is widely used as acid catalyst in alkylation, acylation, isomerization, aromatization and other reactions [1–4]. However, the diffusion limitations caused by the small pore apertures that transport guest molecules to the active sites inside zeolites have restricted the catalytic activity of zeolites for various catalytic reactions. In order to overcome these diffusion limitations, many studies have focused on how to decrease the size or thickness of zeolite crystals, ensuring that diffusion paths are kept short and more active sites are exposed to guest molecules for a given mass of zeolite material.

Compared with the micro-sized zeolites, nano-crystalline zeolites have a larger external surface area and better accessibility to internal micropores, which

could be advantageous properties in catalysis applications, especially in some reactions with severe coking [5].

It is well-known that aromatization of olefins undergo many reactions over the zeolites, such as cracking, oligomerization, isomerization, cyclization, as well as hydrogen transfer over the Brønsted and Lewis acid sites of the zeolite [6]. The aromatization of olefins is of great significance both in the theoretical and chemical industrial fields for synthetic resin, rubber, solvent, detergent, clean gasoline and other chemical intermediates, etc [7,8]. Outstanding aromatization performances have been observed over the ZSM-5 zeolite modified with the incorporation of Zn in terms of the selectivity and stability compared with the conventional MFI zeolites, which could be attributed to the fact that the modified Zn influenced the acidity of zeolites effectively.

Zn-containing ZSM-5 can be prepared by incipient wetness impregnation, ion exchange in aqueous solution,

chemical vapor deposition, and isomorphous substitution techniques. Compared with the conventional incipient wetness impregnation method, the in-situ synthesis of heteroatomic zeolites substituted with Zn (nano-ZSM-5 zeolites) made the Zn species have a higher diffusion and stability.

In this work, the Zn-modified nano-ZSM-5 zeolites were prepared by incipient wetness impregnation and isomorphous substitution. The effects of the Zn-modification method on the acidity and catalytic performance in aromatization of 1-hexene over the nano-ZSM-5 zeolite were also studied.

2 Experimental

2.1 Preparation of nano-ZSM-5 zeolite parent and isomorphously substituted by zinc samples

The nano-ZSM-5 zeolite sample was synthesized according to Ref. [9]. The molar ratio of initial mixtures was $n(\text{Al}_2\text{O}_3):n(\text{SiO}_2):n(\text{Na}_2\text{O}):n(\text{H}_2\text{O})=2.5:100:4:2500$. Sodium aluminates (NaAlO_2), distilled water, and NaOH were mixed homogeneously with agitation, and then silica gel (30% SiO_2 in water) solution was slowly dropped into the mixture of NaAlO_2 and NaOH with vigorous stirring. The 5.0% (mass fraction) seed suspension was then added to the reaction mixture and stirred for 10 min. A hydrothermal treatment was later performed at 180 °C for 24 h. The obtained solid was washed with distilled water, dried at 110 °C, exchanged by a 0.5 mol/L NH_4NO_3 and then calcined at 550 °C for 3 h in air to obtain the H-form products. The as-synthesized samples were denoted as HNZ5.

The samples $x\text{Zn}/\text{HNZ5}$ were prepared by the conventional impregnation methods with $\text{Zn}(\text{NO}_3)_2$ solution which was finally converted into $x\text{ZnO}$, $x=3\%$, 5%.

The nano-ZSM-5 zeolites isomorphously substituted by Zn were in-situ synthesized based on the seed-induced method without organic templates by a gel consisting of zinc nitrate, sodium aluminate, silicasol, sodium hydroxide, and deionized water. The molar composition of gel was $n(\text{ZnO}):n(\text{Al}_2\text{O}_3):n(\text{SiO}_2):n(\text{Na}_2\text{O}):n(\text{H}_2\text{O})=y/2:1:40:6:1250$ ($y=n(\text{Zn})/n(\text{Al})$). Then, 2% (mass fraction) seed solution was added with vigorous stirring. The mixture was heated at 180 °C for 24 h. The residuums were washed, dried, exchanged by NH_4NO_3 and then calcined to obtain the H-form of the samples. The obtained samples were labeled as $y\text{Zn}/\text{Al-HNZ5}$ ($y=0.25, 0.60$).

2.2 Characterization

Powder X-ray diffraction (XRD) patterns of the prepared samples were recorded on a Bruker D8 advance diffractometer using Cu K_α ($\lambda=1.5404 \text{ \AA}$) irradiation at

40 kV and 40 mA with a Lynx eye detector in the 2θ range of 5°–55°. IR spectroscopies of adsorbed pyridine (Py-IR) analysis of samples were measured on a PE100 FTIR spectrometer equipped with a high temperature flow cell with CaF_2 windows. Pyridine adsorption was carried out by dropwise injections of purified pyridine (up to 10 μL) using a microliter syringe into the gas line through a septum injection port at 423 K followed by desorption of the pyridine in a vacuum at 150 °C. All spectra were recorded at 20 °C. The relative amount of Brönsted acid sites (BAS) and Lewis acid sites (LAS) was estimated based on the squares of the corresponding signals in the IR spectra in the range of 1400–1600 cm^{-1} using the integrated molar absorption coefficients reported by EMEIS [10]. N_2 adsorption–desorption characterization of the prepared ZSM-5 molecular sieves (t-plot pore volume, BET surface area) was performed at 77 K using an Autosorb–1–MP apparatus (Quantachrome Instruments). Prior to the adsorption measurements, each sample was degassed under a vacuum of $1.33 \times 10^{-3} \text{ Pa}$ at 300 °C for 12 h. The crystal morphology and size of ZSM-5 powders were observed by scanning electron microscope (SEM) (JSM–6480A, Japan). NH_3 -TPD experiments were carried out on a conventional setup equipped with a thermal conductivity detector. TPD profiles were obtained in a temperature range from 120 °C to 600 °C at a constant heating rate of 15 °C/min in a 40 mL/min flow of helium. The chemical compositions of the samples were determined by X-ray fluorescence (XRF) spectroscopy on a Bruker SRS–3400 instrument.

The 1-hexene aromatization was employed to evaluate the performance of the synthesized zeolite samples. The reaction was performed in a continuous flow high-pressure fixed-bed micro-reactor under the conditions of $t=480 \text{ °C}$, $p=0.5 \text{ MPa}$, $\text{WHSV}=2.0 \text{ h}^{-1}$ and $Q_{\text{N}_2}=75 \text{ mL/min}$. 1 g catalyst was loaded in the middle part of a fixed-bed stainless reactor with 600 mm in length and 10 mm in diameter, and then activated at 500 °C for 1 h in nitrogen flow prior to the reaction. 1-hexene was introduced when the temperature dropped to 480 °C. Both gas and liquid products were collected, followed by being analyzed using a Techcomp GC7900 with a PONA capillary column and a flame ionization detector.

3 Result and discussion

3.1 Catalyst characterization

The XRD patterns of the ZSM-5 zeolite sample HNZ5 and isomorphously substituted by Zn are shown in Fig. 1. Every sample showed the characteristic patterns of MFI topological structures. The intensity of the peaks of the zeolites decreased with the increase of Zn content,

indicating that low crystallization caused by the formation of extraframework species would occur because of difficult incorporation of Zn into the framework of the zeolite. Moreover, no diffraction peaks of ZnO crystallites in ZSM-5 zeolites isomorphously substituted by Zn were observed [11,12], indicating that the Zn species in the samples were highly dispersed. In addition, half band width of γ Zn/Al-HNZ5 samples became wider with the increase of Zn content, which could be explained by the decrease of the particle size of the samples due to Zn incorporation.

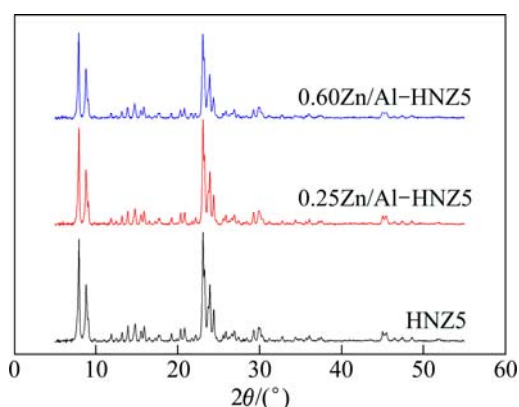


Fig. 1 XRD patterns of nano-ZSM-5 zeolite parent and samples isomorphously substituted by Zn

The morphologies of HNZ5 and isomorphously substituted samples γ Zn/Al-HNZ5 with different Zn contents were investigated by SEM (Fig. 2). It can be seen that the crystal morphology of the nano-ZSM-5 crystals includes large orthogonal shape polycrystalline agglomerates, and individual crystal of these agglomerates is composed of nanosized crystals with size of 100–200 nm. The samples isomorphously substituted by Zn (γ Zn/Al-HNZ5) also show large agglomerates with irregular blocky morphology composed of nanocrystals with size of 50–100 nm, indicating that the synthesized zeolites are nanoscale materials. Evidently, this indicates that the introduction of Zn had an apparent effect on the crystal morphology of ZSM-5 zeolite. Furthermore, these primary crystal particles and their agglomerates vary slightly with the change of Zn content in the samples.

Figure 3 provides the N_2 adsorption–desorption isotherms for samples with different Zn contents. The textural properties of all samples are given in Table 1. As illustrated in Fig. 3, the isotherms of HNZ5, modified samples 3Zn/HNZ5 and 5Zn/HNZ5 were type I isotherms with a plateau at high relative pressures $p/p_0 > 0.9$, which is the characteristic of microporous materials with limited interparticle space (textural mesoporosity). Contrary to these samples, apparent hysteresis appeared in the relative pressure (p/p_0) range

from 0.4 to 1.0 for the nano-ZSM-5 zeolites isomorphously substituted by Zn, indicating that more intergranular mesopores were formed among smaller particles [13], which could also be supported by the results of XRD and SEM results. Compared with the

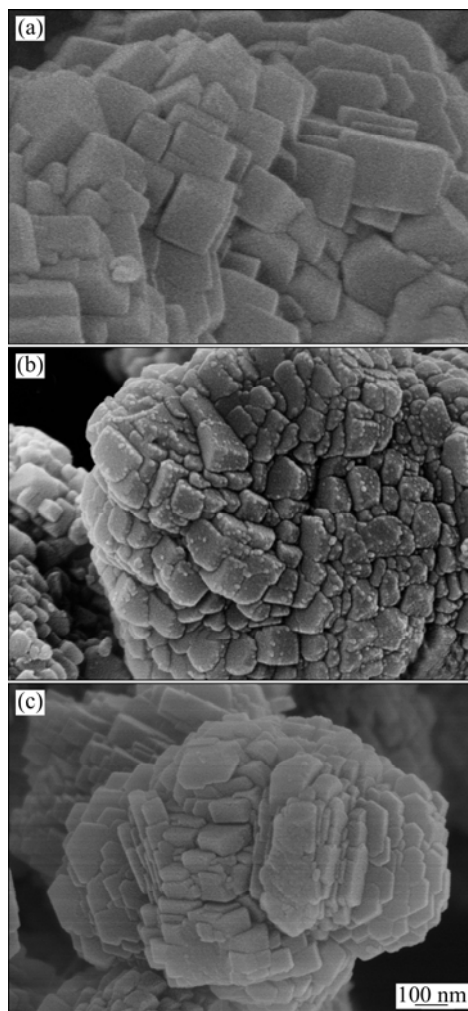


Fig. 2 SEM images of nano-ZSM-5 zeolite parent and Zn-modified samples: (a) HNZ5; (b) 0.25Zn/Al-HNZ5; (c) 0.60Zn/Al-HNZ5

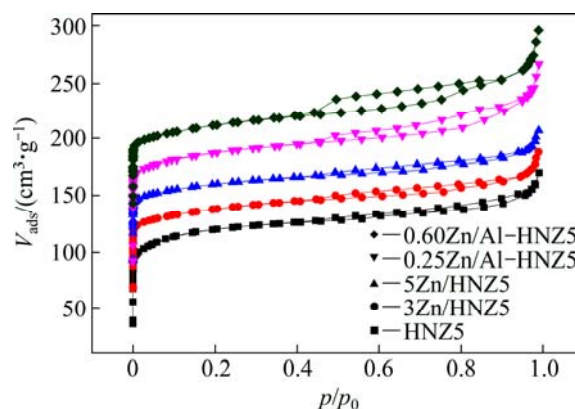


Fig. 3 N_2 adsorption–desorption isotherms of nano-ZSM-5 zeolite parent and Zn-modified samples

isotherms of the HNZ5, for the samples isomorphously substituted by Zn and Zn-supported by impregnation methods at relative pressure (p/p_0) between 0 and 0.2, the amount of N_2 adsorption decreased with the increase of Zn content in the products. Correspondingly, the micropore volume of ZSM-5 zeolite was reduced from 0.153 to 0.116 cm^3/g , as revealed in Table 1. The micropore volume decreased with the increase of Zn content for samples $xZn/HNZ5$, which could be ascribed to the blockage of part micropores occurring in the impregnation process with high content of Zn. The incorporation of Zn by isomorphously substituted method reduced the crystallization and produced a certain amount of amorphous species which blocked the micropore of the zeolites, resulting in the decrease of micropore volume of the samples $xZn/Al-HNZ5$. Compared with the decrease of micropore volume, the mesopore volume of the Zn-modified samples was significantly increased from 0.110 to 0.173 cm^3/g , which could be attributed to the decrease of particle size and formation of more intergranular mesopores.

When Zn was incorporated into ZSM-5 zeolites by incipient wetness impregnation, both the micropore and mesopore volumes decreased clearly with the increase of Zn content, because the particles of ZnO filled into the intergranular mesoporous and blocked the micropore of the zeolites.

A change in the acidic properties is usually evaluated by the temperature-programmed desorption of ammonia, and the profiles can be differentiated both by the integral of the profiles and by the shift in the peak temperature. The former corresponds to the amount of acidic sites, and the latter indicates the strength of the acidic sites. NH_3 -TPD profiles of the nanoscale HZSM-5 zeolite and the Zn-modified samples were illustrated in Fig. 4, and the data of acidity are listed in Table 1. Two typical NH_3 desorption peaks are observed over the profile of HNZ5 sample. One peak is centred at 226 °C, the other is centred at 434 °C, corresponding to weak and strong acid sites, respectively. When Zn was incorporated by incipient wetness impregnation, both peaks were widened, and the intensity of the peak for strong acid sites was obviously reduced. As shown in

Fig. 4, there were obvious shifts toward higher temperatures for the low-temperature desorption peaks and toward lower temperatures for the high-temperature desorption peaks on the NH_3 -TPD profiles with increasing Zn-loading. The peak for weak acid sites of 5Zn/HNZ5 shifted to the higher temperature of 254 °C, while that for strong acid sites shifted to the lower temperature of 408 °C. All these changes suggested that the strong acid sites were eliminated and some weak acid sites were newly formed. The nano-ZSM-5 zeolites isomorphously substituted by Zn exhibited similar regularity as the incipient wetness impregnation samples, which could be ascribed to that the framework aluminium atoms which provided Brønsted acid sites were isomorphously substituted by Zn and exhibited weak Brønsted acidity. Many extra framework Zn species existed in $yZn/Al-HNZ5$ samples due to the low crystallization, which exhibited similar conditions in the samples $xZn/HNZ5$. In addition, the smaller BET surface area and more amorphous species led to the lower acid density of 0.60Zn/Al-HNZ5.

The Py-IR experiments assisted the identification of the Lewis and Brønsted acid sites of the ZSM-5 zeolites. According to previous reports on pyridine chemisorption [14], in Fig. 5, the bands at ~ 1540 and ~ 1450 cm^{-1} belong exclusively to Brønsted sites and Lewis sites, respectively, while the band at ~ 1490 cm^{-1} is attributed to both the Brønsted acid and Lewis acid sites. To investigate the specific changes in the Brønsted and the Lewis acid sites of the ZSM-5 zeolites with different Zn-loading contents and modified by different methods, we took the ratios of the peak intensities at ~ 1540 and ~ 1450 cm^{-1} (B/L ratio) in the Py-IR spectra as a means of comparing the relative amount of the Brønsted and Lewis acid sites in the samples. An extinction coefficient of 1.50 was adopted according to Ref. [15]. The numbers of Lewis and Brønsted sites for the ZSM-5 samples were estimated by combining results from the TPD experiments and these data are presented in Table 1. The changes in the Lewis sites and Brønsted sites were compatible with the changes in weak acidity and strong acidity, although the numbers of Lewis and Brønsted sites were not directly proportional to the numbers of

Table 1 Textural and acid properties of nano-ZSM-5 zeolites parent and Zn-modified samples

Sample	Mass fraction of Zn-loading/%	Surface area/($m^2 \cdot g^{-1}$)		Pore volume/($cm^3 \cdot g^{-1}$) ²⁾			Acid amount/($mmol \cdot g^{-1}$) ³⁾			B/L ratio ⁴⁾
		S_{BET}	S_{Micro}	V_{Total}	V_{Micro}	V_{Meso}	Total acidity	Weak acidity	Strong acidity	
HNZ5	–	447	373	0.263	0.153	0.110	2.39	1.14	1.25	9.00
3Zn/HNZ5	3.0	408	341	0.245	0.139	0.106	2.14	1.34	0.81	0.47
5Zn/HNZ5	5.0	379	322	0.228	0.131	0.097	1.97	1.36	0.62	0.21
0.25Zn/Al-HNZ5	1.6 ¹⁾	400	325	0.288	0.135	0.153	2.35	1.37	0.98	2.18
0.60Zn/Al-HNZ5	3.4 ¹⁾	359	280	0.279	0.116	0.173	1.54	0.86	0.68	0.62

1) Determined by XRF; 2) Determined by N_2 adsorption–desorption at $p/p_0=0.99$; 3) Determined by NH_3 -TPD; 4) Determined by Py-IR

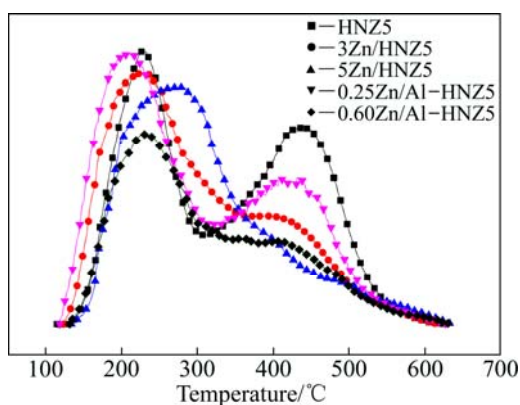


Fig. 4 NH_3 -TPD profiles of nano-ZSM-5 zeolite parent and Zn-modified samples

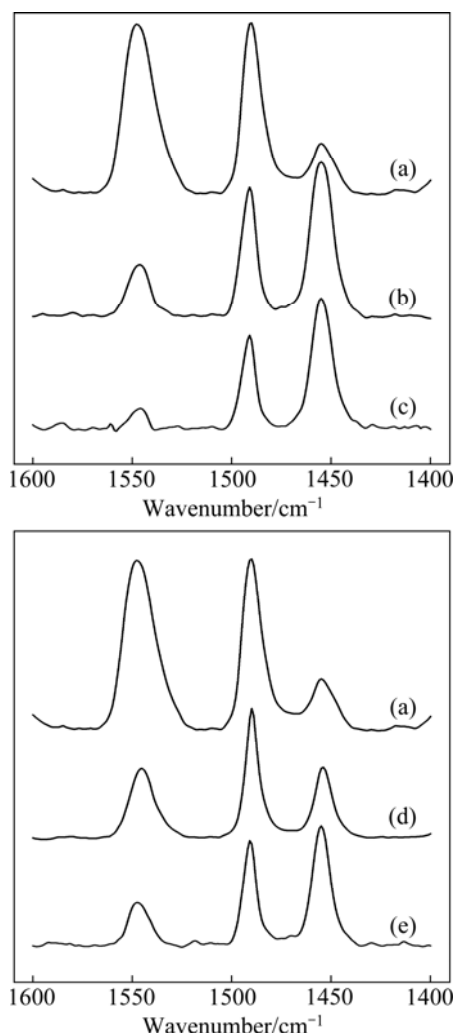


Fig. 5 Py-IR spectra of nano-ZSM-5 zeolite parent and Zn-modified samples: (a) HNZ5; (b) 3Zn/HNZ5; (c) 5Zn/HNZ5; (d) 0.25Zn/Al-HNZ5; (e) 0.60Zn/Al-HNZ5

weak acid sites and strong acid sites, respectively. Obviously, the Brønsted acid sites were dominant over the parent sample HNZ5, and the B/L ratio was 9.00. In the presence of either isomorphous substitution or

incipient wetness impregnation, the acid site distribution of zeolite was clearly varied with the incorporation of Zn. The Brønsted acid sites were reduced and some new Lewis acid sites were formed after the incorporation of Zn. This can be determined that the extra framework Zn species combined with the Brønsted acid sites and [Al–O–Zn–O–Zn–O–Al] or [Al–O–Zn–O–Al] species formed, which acted as the Lewis acid sites [16].

As shown in Table 1, sample 0.60Zn/Al-HNZ5 with Zn-loading amount of 3.4% has a higher B/L ratio of 0.62 than the sample 3Zn/HNZ5 with Zn-loading amount of 3% and B/L ratio of 0.47. Combining the Zn-loading with Py-IR results, the Zn species formed more Lewis acid sites at the expense of Brønsted ones by the incipient wetness impregnation method than the isomorphous substitution with the similar Zn-loading. It can be ascribed to that more Zn species were loaded on the extra surface area on the condition of the incipient wetness impregnation method and some Zn species were inserted into the framework of the zeolites by isomorphous substitution at the same time.

3.2 Catalytic performances

The nano-ZSM-5 zeolite and Zn-modified samples by different methods were applied to 1-hexene aromatization to evaluate the catalytic performance under the conditions of $t=480\text{ }^\circ\text{C}$, $p=0.5\text{ MPa}$, $\text{WHSV}=2.0\text{ h}^{-1}$ and $Q_{\text{N}_2}=75\text{ mL/min}$, and the results are shown in Fig. 6. As for the product, only trace amount of 1-hexene was found, indicating that the conversion rate of 1-hexene was approximately 100% over every catalyst.

As shown in Fig. 6, the aromatic yield over the sample HNZ5 decreased from 47.9% to 29.2% with the time on steam (TOS) increasing from 2 to 10 h, indicating the quick deactivation of the catalyst. When Zn was incorporated into ZSM-5 zeolites, the 1-hexene aromatization stabilities were significantly improved, particularly over the samples of 3Zn/HNZ5 and

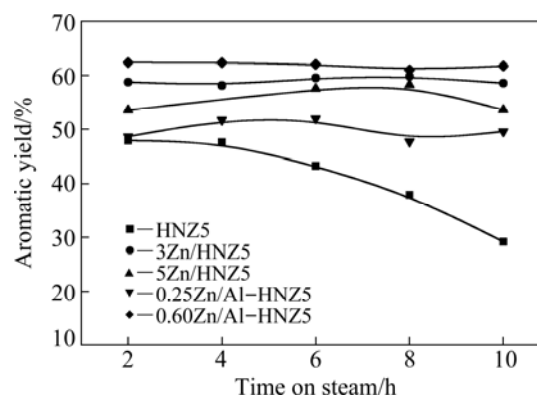


Fig. 6 Aromatic yield of 1-hexene over nano-ZSM-5 zeolite parent and Zn-modified samples

0.60Zn/Al–HNZ5 due to the suitable Zn-loading. The aromatic yield almost did not reduce in 10 h for the two catalysts. These results demonstrated that Zn species promoted the aromatization greatly.

It is well-known that the aromatization required the synergistic effect of Brønsted and Lewis acid sites. The process of olefins transformed to aromatics over the zeolites consisted of many reactions, such as cracking, oligomerization, isomerization, cyclization, and hydrogen transfer, over the Brønsted acid sites via the carbenium ion intermediates, and that the aromatics were formed over HZSM-5 zeolites mainly through the hydrogen transfer reactions [7]. The incorporation of zinc species into the ZSM-5 zeolite provided many Lewis acid sites as the hydrogen transfer active sites and reduced the excess Brønsted acid sites, which can increase the aromatic yield.

For the incipient wetness impregnation samples, the B/L ratios of 3Zn/HNZ5 and 5Zn/HNZ5 reduced to 0.47 and 0.21, respectively, and the aromatic yield was increased and the reaction stability was improved evidently compared with nano-ZSM-5 zeolite parent. This evidenced that the decreased B/L ratio contributed to increase of aromatization selectivity.

As the B/L ratios reduced from 9.00 to 0.62 for the sample 0.60Zn/Al–HNZ5 modified by isomorphous substitution method and the short diffusion path of feed/products, the synergistic effect of Brønsted and Lewis acid sites was improved obviously, hence the aromatic yield of 1-hexene aromatization over the 0.60Zn/Al–HNZ5 sample reached the maximum compared with all other samples.

4 Conclusions

1) The nano-ZSM-5 zeolites isomorphously substituted by Zn in-situ were synthesized by a seed-induced method without organic templates. The incorporation of Zn could decrease the particle size of zeolite crystals and result in larger intergranular mesopore.

2) Compared with Zn-modified samples by incipient wetness impregnation method, the nano-ZSM-5 zeolites isomorphously substituted by Zn exhibited higher dispersion of Zn species, which could significantly promote the synergetic effect between the Brønsted and Lewis acid sites.

3) The reaction stability and aromatization selectivity for 1-hexene aromatization were dramatically improved for the nano-ZSM-5 zeolites isomorphous substituted by Zn. The highest selectivity of 62.4% for 1-hexene aromatization was obtained for the sample 0.60Zn/Al–HNZ5.

References

- [1] SNYDER M A, TSAPATSIS M. Hierarchical nanomanufacturing: From shaped zeolite nanoparticles to high-performance separation membranes [J]. *Angewandte Chemie International Edition*, 2007, 46(40): 7560–7573.
- [2] TANAKA Y, SAWAMURA N, IWAMOTO M. Highly effective acetalization of aldehydes and ketones with methanol on siliceous mesoporous material [J]. *Tetrahedron Letters*, 1998, 39(51): 9457–9460.
- [3] TAO Y S, KANO H, ABRAMS L, KANEKO K. Mesopore-modified zeolites: Preparation, characterization, and applications [J]. *Chemical Reviews*, 2006, 106(3): 896–910.
- [4] CORMA A, DÍAZ-CABAÑAS M J, JORDÁ J L, MARTINEZ C, MOLINER M. High-throughput synthesis and catalytic properties of a molecular sieve with 18- and 10-member rings [J]. *Nature*, 2006, 443(7113): 842–845.
- [5] CHENG Y, LIAO R H, LI J S, SUN X Y, WANG L J. Synthesis research of nanosized ZSM-5 zeolites in the absence of organic template [J]. *Journal of Materials Processing Technology*, 2008, 206(1): 445–452.
- [6] LI Y N, LIU S L, XIE S J, XU L Y. Promoted metal utilization capacity of alkali-treated zeolite: Preparation of Zn/ZSM-5 and its application in 1-hexene aromatization [J]. *Applied Catalysis A: General*, 2009, 360(1): 8–16.
- [7] NI You-ming, SUN Ai-ming, WU Xiao-ling, HU Jiang-lin, LI Tao, LI Guang-xing. Aromatization of methanol over La/Zn/HZSM-5 catalysts [J]. *Chinese Journal of Chemical Engineering*, 2011, 19(3): 439–445.
- [8] ZHANG K, LIU Y Q, TIAN S, ZHAO E H, ZHANG J C, LIU C G. Preparation of bifunctional NiPb/ZnO–diatomite–ZSM-5 catalyst and its reactive adsorption desulfurization coupling aromatization performance in FCC gasoline upgrading process [J]. *Fuel*, 2013, 104: 201–207.
- [9] WU Wei, WANG Xin. A method of preparing nona-ZSM-5: CN, 101643219 [P]. 2010–02–10. (in Chinese)
- [10] EMEIS C A. Determination of integrated molar extinction coefficients for infrared absorption bands of pyridine adsorbed on solid acid catalysts [J]. *Journal of Catalysis*, 1993, 141(2): 347–354.
- [11] XU Dong, CHENG Xiao-nong, YAN Xue-hua, XU Hong-xing, SHI Li-yi. Sintering process as relevant parameter for Bi₂O₃ vaporization from ZnO–Bi₂O₃-based varistor ceramics [J]. *Transactions of Nonferrous Metals Society of China*, 2009, 19(6): 1526–1532.
- [12] ZHU Jian-yu, ZHANG Jing-xia, ZHOU Hui-fen, QIN Wen-qing, CHAI Li-yuan, HU Yue-hua. Microwave-assisted synthesis and characterization of ZnO-nanorod arrays [J]. *Transactions of Nonferrous Metals Society of China*, 2009, 19(6): 1578–1582.
- [13] NI Y M, SUN A M, WU X L, HAI G L, HU J L, LI T, LI G X. The preparation of nano-sized H [Zn, Al] ZSM-5 zeolite and its application in the aromatization of methanol [J]. *Microporous and Mesoporous Materials*, 2011, 143(2): 435–442.
- [14] ZHU X X, LIU S L, SONG Y Q, XIE X J, XU L Y. Catalytic cracking of 1-butene to propene and ethene on MCM-22 zeolite [J]. *Applied Catalysis A: General*, 2005, 290(1): 191–199.
- [15] EMEIS C A. Determination of integrated molar extinction coefficients for infrared absorption bands of pyridine adsorbed on solid acid catalysts [J]. *Journal of Catalysis*, 1993, 141(2): 347–354.
- [16] BISCARDI J A, MEITZNER G D, IGLESIA E. Structure and density of active Zn species in Zn/H–ZSM5 propane aromatization catalysts [J]. *Journal of Catalysis*, 1998, 179(1): 192–202.

Zn 改性纳米 ZSM-5 分子筛的制备及其催化己烯-1 芳构化反应性能

王高亮¹, 吴伟¹, 昝望¹, 白雪峰¹, 王文静¹, 戚鑫¹, O.V. KIKHTYANIN²

1. 黑龙江大学 化学化工与材料学院, 高效转化的化工过程与技术黑龙江省普通高校重点实验室, 哈尔滨 150080;
2. Boreskov Institute of Catalysis, Siberian Branch of the Russian Academy of Sciences, Novosibirsk 630090, Russia

摘要: 研究以浸渍法和同晶置换法引入 Zn 对纳米 ZSM-5 分子筛催化己烯-1 芳构化反应性能的促进作用。采用无模板剂的晶种引导法合成具有纳米尺度的 ZSM-5 分子筛。分别以传统浸渍法和同晶置换法制备 Zn 改性的纳米 ZSM-5 分子筛催化剂 $x\text{Zn}/\text{HNZ5}$ 和 $y\text{Zn}/\text{Al-HNZ5}$ 。采用 XRD、XRF、 N_2 物理吸附、SEM、 NH_3 -TPD 和 Py-IR 等分析手段对所制备样品的结构、化学组成以及酸性进行表征, 并在 $480\text{ }^\circ\text{C}$ 和质量空速为 2.0 h^{-1} 的条件下对其催化己烯-1 芳构化性能进行考察。与 $x\text{Zn}/\text{HNZ5}$ 相比, $y\text{Zn}/\text{Al-HNZ5}$ 表现出更小的粒径尺寸和更高的 Zn 物种分散度, 使其具有更大的晶间介孔和更均匀的酸中心分布。催化性能评价结果表明, Zn 同晶置换改性的纳米 ZSM-5 分子筛具有更好的 Brønsted 和 Lewis 酸中心协同作用, 能够显著地提高纳米 ZSM-5 分子筛的催化己烯-1 芳构化反应收率和稳定性。

关键词: 纳米 ZSM-5 分子筛; Zn 改性; 催化性能; 同晶置换; 芳构化反应

(Edited by Wei-ping CHEN)